AIChE

Elucidation of the Interaction Among Cellulose, Xylan, and Lignin in Steam Gasification of Woody Biomass

Chihiro Fushimi
Collaborative Research Center for Energy Engineering, Institute of Industrial Science, The University of Tokyo, Meguro-ku, Tokyo 153-8505, Japan

Shingo Katayama, Kazuhiko Tasaka, and Masahiro Suzuki
Dept. of Chemical System Engineering, The University of Tokyo, Bunkyo-ku, Tokyo 113-8656, Japan

Atsushi Tsutsumi
Collaborative Research Center for Energy Engineering, Institute of Industrial Science, The University of Tokyo, Meguro-ku, Tokyo 153-8505, Japan

DOI 10.1002/aic.11705
Published online December 24, 2008 in Wiley InterScience (www.interscience.wiley.com).

The reaction mechanism for gas and tar evolution in the steam gasification of cellulose, lignin, xylan, and real biomass (pulverized eucalyptus) was investigated with a continuous cross-flow moving bed type differential reactor, in which tar and gases can be fractionated according to reaction time. In the steam gasification of real biomass, the evolution rates of water-soluble tar (derived from cellulose and hemicelluloses) and water-insoluble tar (derived from lignin) decrease with increasing reaction time. It was found that the evolution of water-soluble tar occurs earlier than in the gasification of pure cellulose, indicating an interaction of the three components. The predicted yield of water-insoluble tar is substantially less than that of real biomass. This implies that the evolution of tar from the lignin component of biomass is enhanced, compared with pure lignin gasification, by other components. The gas evolution rate from real biomass is similar to that predicted by the superposition of cellulose, lignin, and xylan.
 AIChE J, 55: 529–537, 2009
Keywords: woody biomass, cellulose, xylan, lignin, steam gasification, interaction, tar, continuous cross-flow moving bed type differential reactor

Introduction

The steam gasification of biomass is a promising technology for thermochemical hydrogen production from biomass. Because biomass is a renewable and clean energy resource, biomass-derived hydrogen is essential for a sustainable society.[1] However, during biomass gasification, a large amount of tar is produced, causing problems such as pipeline plugging, defluidization, and a reduction in thermal efficiency.[2] Thus, it is essential to elucidate the reaction mechanism of tar production in gasification for improvements in the controllability and thermal efficiency of biomass gasification systems.

So far, many researchers have conducted experimental studies on the pyrolysis of biomass and examined product

Correspondence concerning this article should be addressed to C. Fushimi at fushimi@iis.u-tokyo.ac.jp.

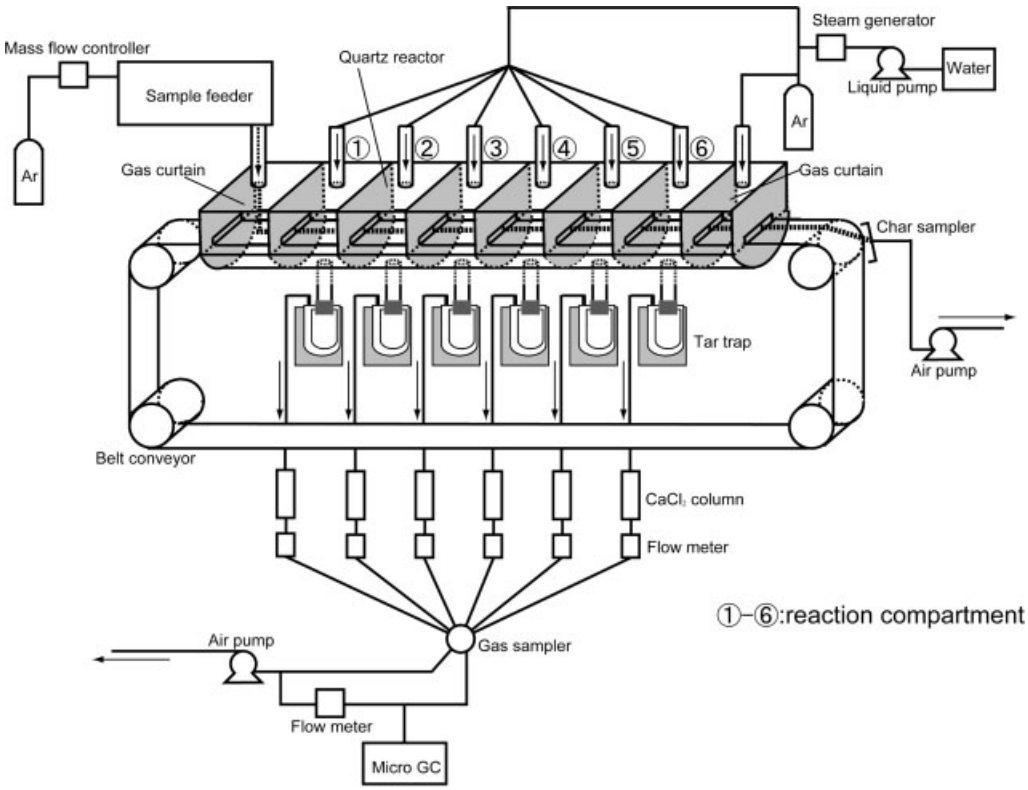

Figure 1. Experimental apparatus.

distribution and kinetics.[3–38] Cellulose has been the most studied. The Broido–Shafizadeh model was the initially proposed mechanism for the pyrolysis of cellulose.[3–5] This model consists of three coupled first-order reactions. The first stage of pyrolysis involves no weight loss and leads to the formation of an intermediate referred to as active cellulose. This is followed by a pair of competing reactions that produce either volatiles or char and gases with weight loss. This concept of active cellulose was inherited in many pyrolysis and gasification models of cellulose proposed later.[6–11,14] Moreover, extensive efforts to explain the intermediate and tar evolution have been reported.[11–14,16–20] Lédé et al.[17] observed that active cellulose is completely soluble in water (anhydro-oligosaccharides).

With regard to the pyrolysis of real biomass, many researchers have studied and proposed reaction models.[21–34] Many of the reaction models assume that the three major components of real biomass (cellulose, hemicellulose, and lignin) are pyrolyzed independently without interaction.[21–23] Yang et al.[21] investigated the roles of the three components in pyrolysis using a thermogravimetric analyzer (TGA). They stated that pyrolysis of the mixed samples indicates negligible interaction among the three components. Svenson and Pettersson stated that calculations in which the results for the three independent materials are added together in the proportions of birch wood have good agreement with birch wood data. This supports the assumption that the three materials act independently during pyrolysis.[22]

On the other hand, some researchers recently reported that the product yield and kinetics of biomass in pyrolysis cannot be explained by the superposition of the values of the three components because of the interaction among the three components during tar production and evolution.[35–38] Hosoya et al. examined the pyrolysis behavior of wood[35,36] and mixtures of cellulose–hemicellulose (glucomannan and xylan) and cellulose–lignin (milled wood lignin)[37] at 1073 K focusing on the behaviors of the wood constituent polymers (cellulose, hemicellulose, and lignin). They reported that the carbonization behavior of the volatile products and the yield of the polysaccharide fraction were not able to be explained as a sum of the pyrolysis of cellulose, hemicellulose, and lignin even after demineralization.[36] They also reported that the interaction between cellulose and lignin considerably affects pyrolysis behaviors, such as those of gas, tar, and char formation and product composition, whereas the cellulose–hemicellulose interaction is not significant.[37] These results motivated us to investigate the interaction among cellulose, lignin, and hemicellulose during tar and gas evolution in the steam gasification of biomass.

Recently, we have developed a continuous cross-flow moving bed type differential reactor (CCDR), in which biomass sample is continuously fed, and the products (tar, gas, and char) can be fractionated in six compartments according to the reaction time.[8] In this experimental apparatus, secondary reactions between volatile matter and char can be minimized because of short residence time. Using this apparatus, we previously studied[8] the mechanism of pyrolysis for cellulose, and found that the dehydration of nascent char takes place after the devolatilization of tar is complete.

In this study, the time profile of tar and gas evolution was investigated in steam gasification of real biomass (pulverized eucalyptus) and its components cellulose, xylan as hemicellu-

Table 1. Elemental Compositions and Ash Content of Samples (wt %)

	Elemental Compositions (Dry, Ash-Free)					Ash			
	C	H	O (Diff.)	N	S	(Dry Basis)	Cellulose	Lignin	Xylan
Cellulose	44.44	6.17	49.39	0	0	0	100	0	0
Lignin	64.47	5.57	26.90	0.15	2.91	17.48	0	100	0
Xylan	40.16	6.12	52.96	0.14	0.62	0.28	0	0	100
Eucalyptus	48.87	6.05	44.17	0.19	0.72	0.43	50	27	23

lose, and lignin. Because it was found that tar evolution takes place mainly at 600–700 K (cellulose) and at 550–773 K (lignin) in our previous study,[7] reaction temperature was set to 673 K. The evolution rates of gas and tar from the real biomass and those predicted by superposition of the data for cellulose, xylan, and lignin were compared to elucidate the interaction among the three components. On the basis of the experimental results, we discuss the reaction mechanism of tar evolution in biomass steam gasification.

Experimental

Apparatus

Schematic image of the CCDR is shown in Figure 1.[8] The reactor consists of a quartz glass half tube covered with a quartz glass plate and a conveyor belt system. The reactor is divided into six compartments (W 90 mm $\times$ D 80 mm $\times$ H 40 mm) where gas flows are independent. The reactor is heated using an infrared gold image furnace (Ulvac Riko Co.). The heating zone of the furnace is divided into a preheating zone and three reaction zones. The temperatures of each reaction zone are measured by K-type thermocouples and independently controlled to be constant at 673 K. Biomass sample is fed out of a feeder onto a conveyor belt made of siliglass (SiO_2 > 96%), which carries the sample across the six compartments, delivering produced char to a char sampling system. The initial time is defined as the time when the sample is fed into the preheating zone. The temperature of each compartment is also measured above the belt (<5 mm) by using other K-type thermocouples. Tar and gases produced in each compartment are sampled with a carrier gas and fractionated according to reaction time. At the end of the conveyor belt, char is collected using the char sampling system. By changing the belt speed, the residence time of each compartment can be varied in the range of 2.4–32 s.

A bowl feeder (model PEF-90AL; Sanki Co.) in an acrylic feeder box was used to feed biomass sample continuously with an Ar carrier gas into the preheating zone through a SUS316 tube (4.35 mm, i.d.). The feed rate was calibrated by weighing the fed sample before and after the experiment and taking the average. Steam was generated in a steam generator and fed into the reactor with Ar carrier gas. Tar evolved in each compartment passed through heated sampling lines, and was then collected separately in six tar traps cooled by ice. Water was eliminated in $CaCl_2$ columns. Although the six sampling lines were gathered in a gas sampler (EMT 4SC6MWE; Valco Instruments Co.), only one of the lines was connected to a micro gas chromatograph (GC) (M-200H; Hewlett Packard Co.). The line to the micro GC was changeable. The flow rate of the effluent gas was measured with a mass flow meter. Using the micro GC, we analyzed H_2, O_2, N_2, CH_4, and CO with an MS-5A column and Ar carrier gas and CO_2, C_2H_4, and C_2H_6 with a Pora Plot Q column and He carrier gas.

Procedure

In this study, Avicel microcrystalline cellulose (Merck Co., <160 μm, Avicel), xylan from birch wood (Sigma-Aldrich Co.), kraft lignin (Kanto Chemical Co., 6.8–160 μm), and pulverized real biomass (Chilean eucalyptus, <500 μm) were used as samples. The elemental compositions and ash content of these samples are shown in Table 1. Each sample was dried at 333 K in an oven for 12 h prior to the experiment. The sample was put in the feeder and the feeder box was purged with Ar. The reactor was also purged with Ar until the concentration of O_2 declined below 1%. The flow rate of the carrier gas in each compartment was then set to 400 N cm^3 min^{-1}. The steam generator, steam feeding lines, and sampling lines were heated to 523, 453, and 423 K, respectively, to avoid the conden-

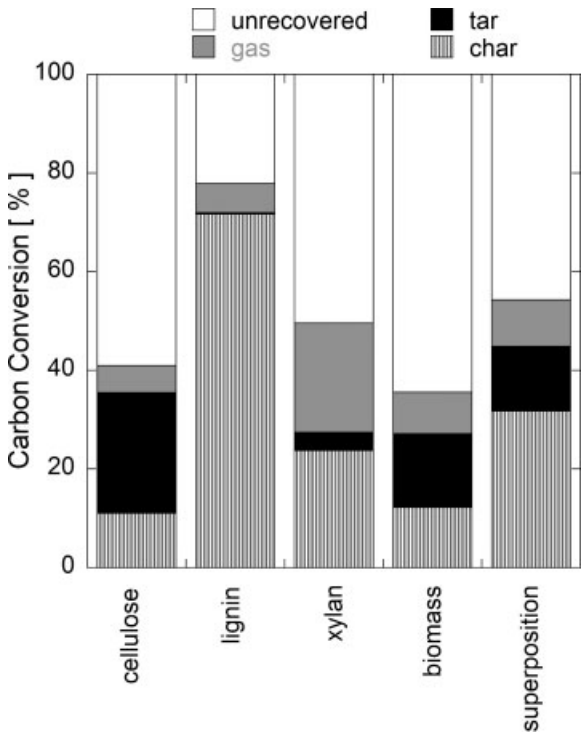

Figure 2. Carbon conversion to gas, tar, and char of each sample.

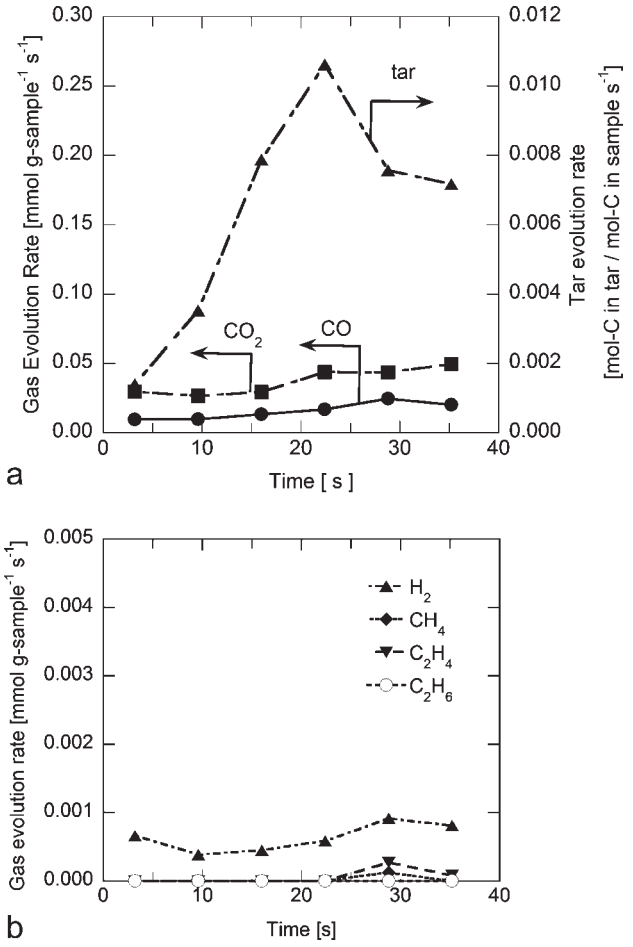

Figure 3. Time profile of gas and tar evolution (cellulose).

sation of steam and tar. After heating the reactor to 673 K, steam (40 vol %) and sample were fed for 60 min. The calibration of the sample feed rate was carried out at room temperature. The sample feed rate was kept at 30–119 mg min^{-1} in this experiment. The belt speed was 750 mm min^{-1}; the corresponding residence time of biomass sample in each compartment was 6.4 s.

Analysis of tar

After the experiment, distilled water was introduced to the reactor and sampling lines to collect water-soluble tar. Deposited tar in the tar traps was collected until the color of the solution became transparent. Acetone was then used as a solvent to extract water-insoluble tar. The molecular weight (MW) of tar was measured using a gel filtration chromatograph (pump: Waters 600E Multi Solvent Delivery System, column: Shodex AsahipakGS-220HQ, detector: Waters 2414 differential refractometer). KCl was added to the solution to reduce the intramolecular ionic repulsion between hydroxyl groups. After evaporating the solvent (water or acetone), the elemental composition of dried tar was analyzed with a CHNS elemental analyzer (2400II CHNS/O; Perkin Elmer). A small amount of the dried tar was milled with KBr (0.1 g) and measured using a Fourier transform infrared (FTIR) spectrometer (FTIR-230; JASCO). The 4000–400 or 4600–400 cm^{-1} wave number range was examined with 16 scans.

In each compartment of the CCDR, the evolution rates of gas and tar were defined as

$$\text{evolution rate (carbon molar basis)} = \frac{M_c}{M \cdot \tau}$$

$$\text{evolution rate (weight basis)} = \frac{M_G}{W \cdot \tau}$$

where M_c, M, τ, M_G, and W represent the molar amount of carbon in the product in a compartment [mol], total molar carbon in fed biomass [mol], residence time in a compartment [s], molar amount of gases in the product in a compartment [mol], and total amount of fed biomass [g], respectively.

Results and Discussion

Trend of gas and tar evolution in gasification of each sample

At first, the temperature profile of the each compartment was measured (not shown). The temperatures were in the

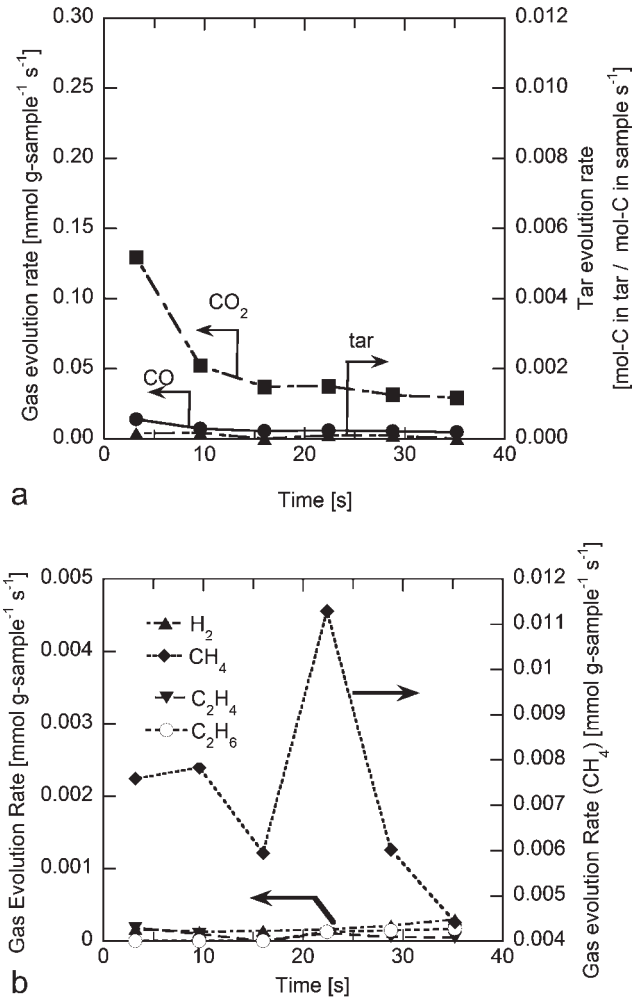

Figure 4. Time profile of gas and tar evolution (lignin).

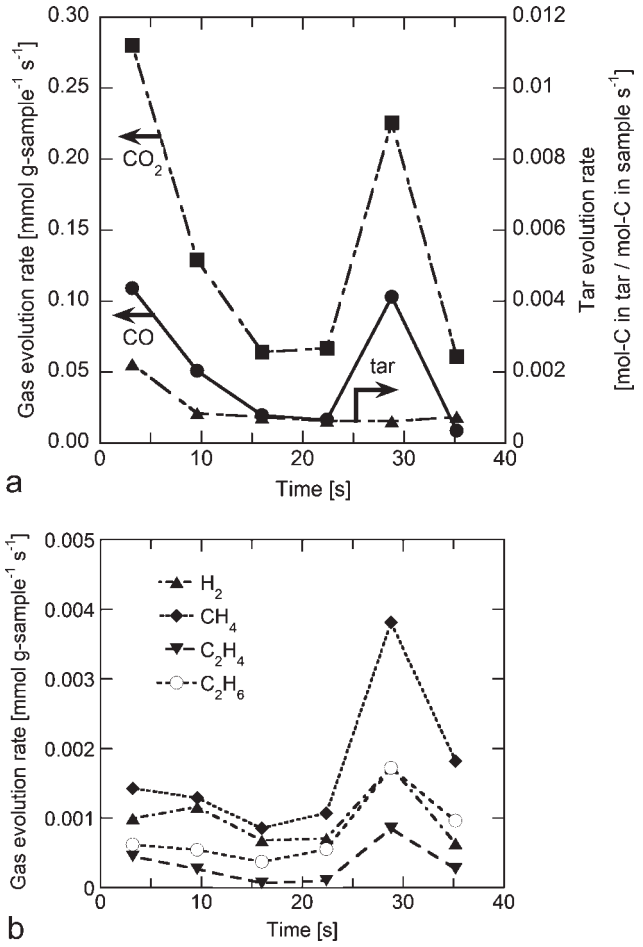

Figure 5. Time profile of gas and tar evolution (xylan).

range of 644–693 K when the set temperatures of the preheating zone and the three reaction zones were 673 K. The average temperature of the six compartments was 675 K.

Figure 2 shows the carbon conversion to gas, tar, and char in steam gasification of cellulose, lignin, xylan, and real biomass. The predicted carbon conversion of biomass, which is calculated by a superposition of carbon conversions for cellulose (50%), lignin (27%), and xylan (23%), is also shown in Figure 2. This ratio of the three main components of the real biomass is obtained by the elemental analysis of biomass using the method reported by Hasegawa et al.[39] Figures 3–6 show the time profiles of evolution rates of CO, CO_2 (mol basis), and tar (carbon molar basis) at 673 K during steam gasification of cellulose, lignin, xylan, and real biomass, respectively. The evolution rates of H_2, CH_4, C_2H_4, and C_2H_6 are also shown in these figures. Figure 7 shows the evolution rate predicted by a superposition of evolution rates for cellulose, lignin, and xylan in the ratio of 50:27:23 by weight. In Figures 3–7, the abscissa represents the elapsed time after the sample was fed onto the quartz belt.

In the case of cellulose (Figure 2), a large amount of tar was produced. All of the collected tar was water-soluble (data are not shown). The amount of char was small. It can be seen from Figure 3 that the tar evolution for cellulose increased rapidly with reaction time and peaked at 22 s. The evolution rate of CO and CO_2 increased slightly with an increase in reaction time to 35 s. These results are attributed to the existence of intermediates.[8] The evolution rates of H_2, CH_4, C_2H_4, and C_2H_6 had similar trends to those of CO and CO_2 although their values were much smaller.

In the case of lignin, ~ 70% of sample converted to char and the amount of tar was very small, as shown in Figure 2. All of the collected tar was water-insoluble (not shown). This is attributed to lignin mainly consisting of hydrophobic aromatic components. It can be seen from Figure 4 that the evolution rates of CO and CO_2 were initially large and decreased with increasing time. This implies that CO and CO_2 are released from lignin and/or nascent char. The evolution rate of CH_4 was much larger than that of cellulose (cf. Figure 3). This is probably due to lignin containing large amounts of methoxyl groups.

For xylan, gas evolution was greater than that of cellulose and lignin, whereas tar evolution for xylan was less than that of cellulose and greater than that of lignin (Figure 2). Dominant tar evolution was observed initially as shown in Figure 5. On the other hand, the time profile of gas evolution had two peaks, initially and at 29 s. This result corresponds to the report by Müller-Hagedorn et al.[28] that showed hemicellulose has two decomposition steps.

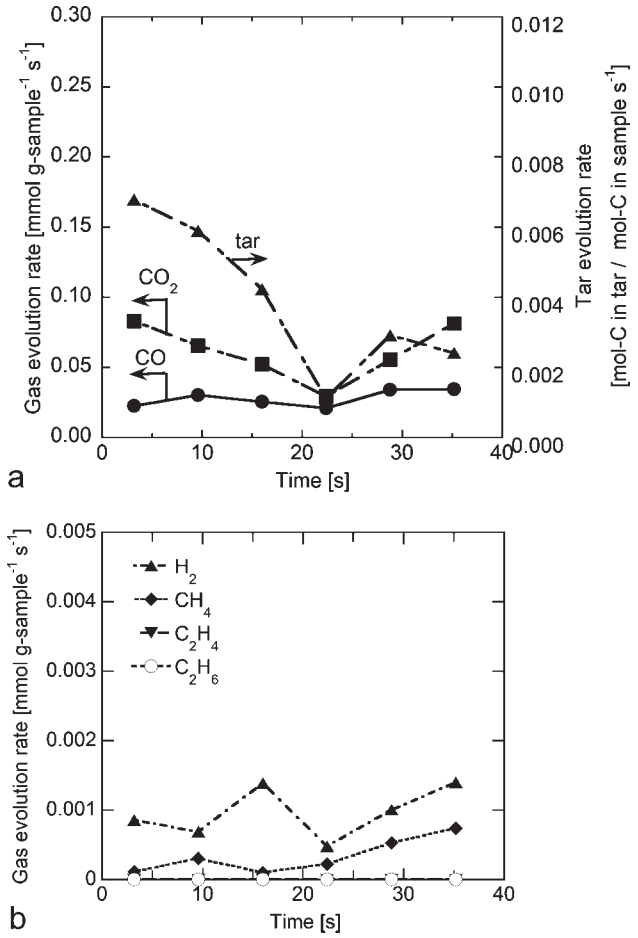

Figure 6. Time profile of gas and tar evolution (biomass: experimental result).

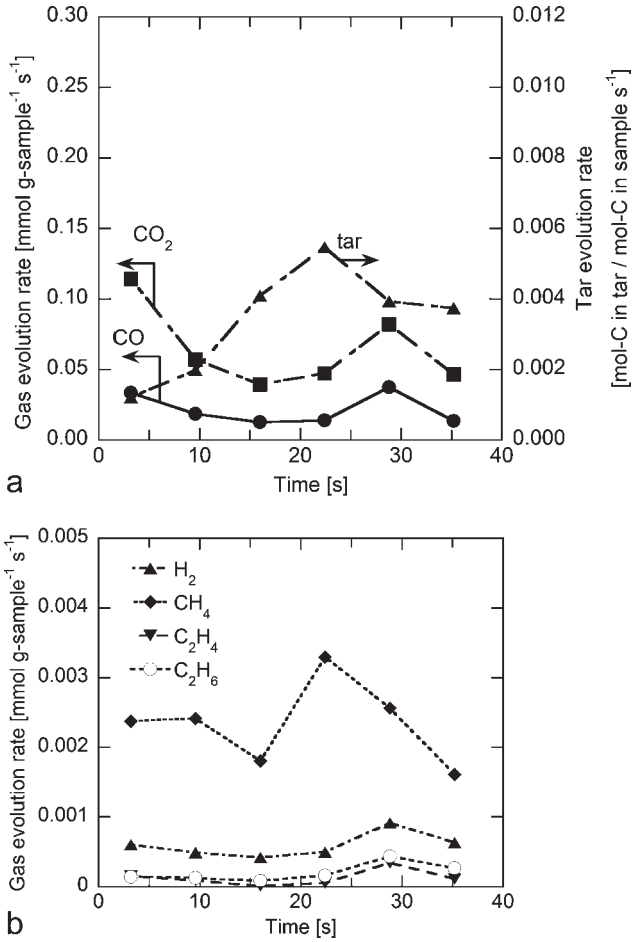

Figure 7. Time profile of gas and tar evolution (biomass: calculated by superposition of cellulose (50%), lignin (27%), and xylan (23%).

In the case of real biomass (Figure 6), a similar trend for tar and gas evolution with xylan gasification was observed. The tar and gas evolution was found to have two peaks, initially and at 29–35 s, indicating a larger amount of gaseous products is derived from xylan in real biomass. The predicted time profile of the gas evolution had two peaks, initially and at 29 s, as shown in Figure 7. This is similar to the time profile of experimental data. However, the tar evolution profile was found to differ for experimental and predicted values. During real biomass gasification, the tar evolution rate was initially a maximum and then a minimum at 22 s. On the other hand, the predicted tar evolution rate increased with time and reached a maximum at 22 s. This result indicates an interaction among the tar components from cellulose, lignin, and xylan.

Figures 8a, b show the amounts of water-soluble and water-insoluble tar in the gasification of real biomass, and the amounts calculated by the superposition of the amounts for the three components, respectively. In the case of real biomass (Figure 8a), both water-soluble and water-insoluble tar evolved initially and the ratio of water-insoluble tar decreased with reaction time. On the other hand, in the calculation (Figure 8b), little water-insoluble tar production was predicted from the superposition of the three components. It is inferred that tar was derived mainly from cellulose because little evolved from lignin and xylan (cf. Figures 2, 4, and 5). These results suggest that in the gasification of real biomass, the amount of water-insoluble tar that mainly evolves from lignin increases and that the evolution of water-soluble tar from cellulose occurs earlier than in the gasification of pure lignin or cellulose.

Analysis of tar

Figure 9 shows the FTIR spectra of water-soluble tar from cellulose, xylan, and biomass (at 3 and 29 s). No significant

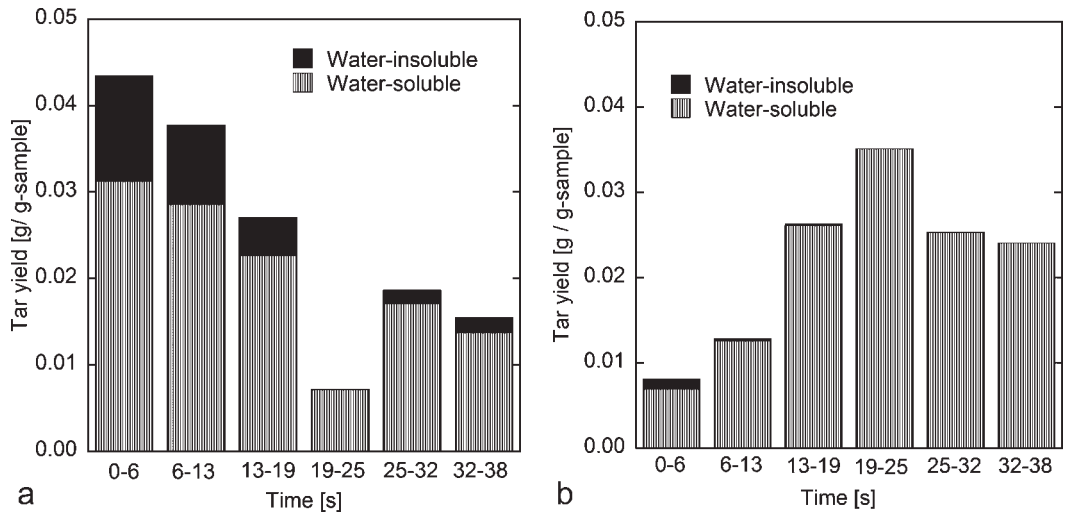

Figure 8. Amount of tar in biomass gasification.

(a) Experiment using real biomass. (b) Calculated by the superposition of cellulose, lignin, and xylan.

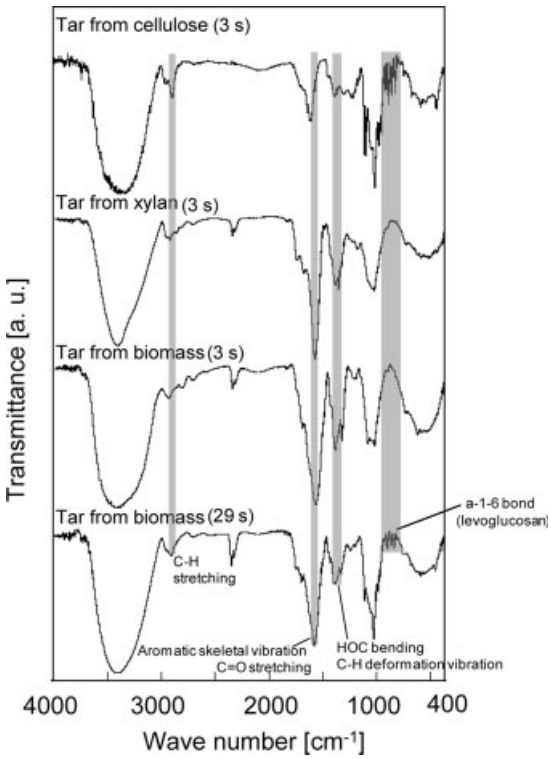

Figure 9. FTIR spectra of water-soluble tar produced from cellulose, xylan, and biomass (reaction time: 3 and 29 s).

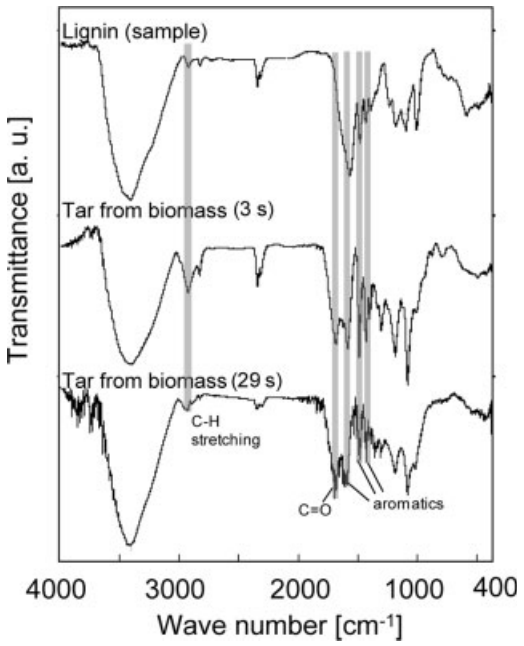

Figure 10. FTIR spectra of lignin and water-insoluble tar produced from biomass (reaction time: 3 and 29 s).

change in the FTIR spectra for tar evolved from cellulose and xylan was observed with reaction time. Every spectrum had small peaks around 2900 cm^{-1}, which can be assigned to C—H stretching in methyl and methylene groups.[40] Tar from cellulose had peaks at 950–800 cm^{-1}. These can be assigned to the α-1-6 bond of levoglucosan, which is the main component of water-soluble tar from cellulose.[3–5] Tar from xylan had strong peaks at around 1400 and 1600 cm^{-1}. The peaks around 1400 cm^{-1} can be assigned to HOC bending and C—H deformation vibration and the peaks around 1600 cm^{-1} can be assigned to C—H and aromatic skeletal vibrations plus C=O stretching.[40] The tar in biomass gasification at 3 s also has comparatively strong peaks around 1400 and 1600 cm^{-1}. On the other hand, tar derived from biomass at 29 s has distinct peaks at 950–800 cm^{-1} and the peaks around 1400 and 1600 cm^{-1} became smaller. Therefore, it can be concluded that in biomass gasification, initially tar is mainly derived from xylan and tar derived from cellulose increases with increasing time at 673 K.

The FTIR spectra of lignin and water-insoluble tar from biomass (3 and 29 s) are shown in Figure 10. The spectrum of lignin had peaks assigned to an aromatic ring at 1600, 1510, 1420 cm^{-1}. Tar from biomass at 3 s also had these peaks. This tar also had a strong peak around 1700–1740 cm^{-1}. This can be assigned to C=O.[40] The spectrum of tar at 29 s had similar peaks to those at 3 s. However, the peaks were smaller. Figure 11 shows the MW distribution of water-insoluble tar from biomass (reaction time: 3 and 29 s) measured by GFC. The MW distribution of tar at 3 s of reaction time had a broad peak at 1000–3000; the tar at 29 s had a much smaller peak of at 1000–3000. Hasegawa et al.[39] reported the MW distribution of tar derived from cellulose has peaks at about 150 and 300 and MW distribution of tar from lignin is distributed at about 1000–4000. The results obtained from FTIR spectra and GFC suggest that the initial water-insoluble tar in biomass gasification contains the component derived from lignin.

From these results, the evolution mechanism of tar and gas in biomass gasification is schematically summarized in Figure 12. Abscissa axes represent elapsed time from the begin-

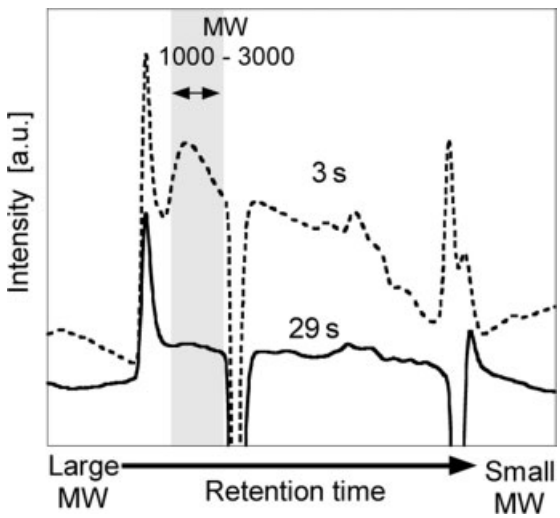

Figure 11. Molecular weight distribution of water-insoluble tar derived from biomass measured by GFC.

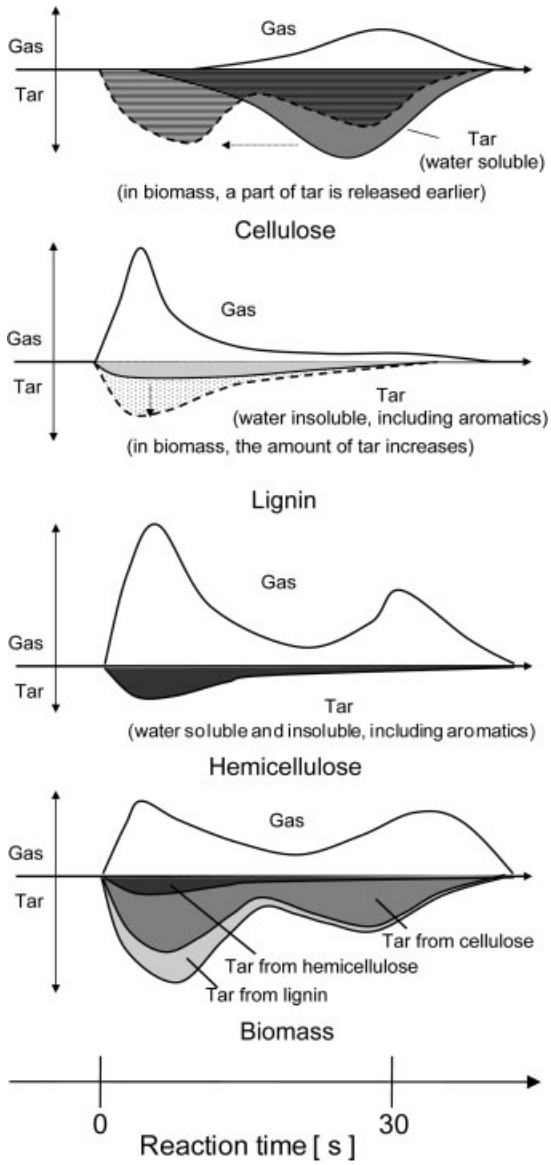

Figure 12. Schematic diagram of gas and tar evolution in biomass gasification at 673 K.

ning of gasification and ordinate axes show evolution rates of gas and tar. For gas, the upper part of the ordinate axes represents larger evolution rates, and for tar the lower part of the axes represents larger evolution rates. In cellulose gasification, tar and gas evolution rates increased with reaction time. The evolutions of tar and gas peaked at about 20 and 30 s, respectively. This indicates the existence of intermediates.[8] On the other hand, in the gasification of real biomass, the evolution of water-soluble tar peaked early. Thus, it can be concluded that tar evolution from cellulose is accelerated by the interaction of the three components, leading to a shift of the tar evolution peak to an earlier stage.

Pure lignin initially releases gas during gasification although the amount is small. Most lignin converts into char. In the gasification of real biomass, however, initially the amount of water-insoluble tar produced is much more than expected from the gasification of pure lignin. Because water-insoluble tar contains aromatic components derived from lignin, it is considered that the evolution of tar from the lignin component of biomass is enhanced, compared with pure lignin gasification, by other components.

Conclusions

Using a CCDR, steam gasification of cellulose, lignin, xylan, and real biomass (pulverized eucalyptus) was investigated at 673 K. It is shown that in real biomass gasification, the evolution rate of gas is similar to that predicted by the superposition of cellulose, lignin, and xylan. On the other hand, the tar evolution rate of real biomass is different from the estimated tar evolution rate using the individual gasification results of the three components. The tar evolution rate from real biomass has two peaks, initially and at 29 s; however, the estimated tar evolution rate has a peak at 22 s. Tar derived from real biomass initially includes both water-soluble tar derived from cellulose and hemicellulose, and water-insoluble tar from lignin. More water-insoluble tar evolves from real biomass than predicted. In the gasification of real biomass, it was found that the evolution of water-soluble tar evolved from cellulose occurs earlier than in the gasification of pure cellulose and that the evolution of water-insoluble tar is enhanced. These results indicate an interaction of the three components.

Acknowledgments

This study was financially supported by a Core Research for Evolutional Science and Technology (CREST) grant from the Japan Science and Technology Agency (JST) and the New Energy and Industrial Technology Development Organization (NEDO). The authors are grateful to Dr. Takeshi Furusawa (Utsunomiya University) and Mr. Yohsuke Yamaguchi for useful discussions and technical support. The authors also acknowledge Mitsubishi Paper Mills Co., Ltd. for providing biomass samples.

Literature Cited

1. Bridgewater AV. The technical and economic feasibility of biomass gasification for power generation. *Fuel*. 1995;74:631–653.
2. Devi L, Ptasinski KJ, Janssen FJJG. A review of the primary measures for tar elimination in biomass gasification processes. *Biomass Bioenergy*. 2003;24:125–140.
3. Shafizadeh F, Lai YZ. Thermal degradation of 1,6-Anhydro-p-β-glucopyranose. *J Org Chem*. 1972;37:278–284.
4. Bradbury AGW, Sakai Y, Shafizadeh F. A kinetic model for pyrolysis of cellulose. *J Appl Polym Sci*. 1979;23:3271–3280.
5. Shafizadeh FJ. Introduction to pyrolysis of biomass. *J Anal Appl Pyrolysis*. 1982;3:283–305.
6. Fushimi C, Araki K, Yamaguchi Y, Tsutsumi A. Effect of heating rate on steam gasification of biomass. I. Reactivity of char. *Ind Eng Chem Res*. 2003;42:3922–3928.
7. Fushimi C, Araki K, Yamaguchi Y, Tsutsumi A. Effect of heating rate on steam gasification of biomass. II. Thermogravimetric-mass spectrometric (TG-MS) analysis of gas evolution. *Ind Eng Chem Res*. 2003;42:3929–3936.
8. Yamaguchi Y, Fushimi C, Tasaka K, Furusawa T, Tsutsumi A. Kinetic study on pyrolysis of cellulose using novel continuous cross-flow moving bed type differential reactor. *Energy Fuels*. 2006;20:2681–2685.
9. Mok WSL, Antal MJ Jr. Effect of pressure on biomass pyrolysis. II. Heat of reaction of cellulose pyrolysis. *Thermochim Acta*. 1983;68:165–186.
10. Cooley S, Antal MJ Jr. Kinetic of cellulose pyrolysis in the presence of nitric-oxide. *J Anal Appl Pyrolysis*. 1988;14:149–161.

11. Banyasz JL, Li S, Lyons-Hart J, Shafer KH. Gas evolution and the mechanism of cellulose pyrolysis. *Fuel*. 2001;80:1757–1763.
12. Li S, Lyons-Hart J, Banyasz JL, Shafer KH. Real-time evolved gas analysis by FTIR method: an experimental study of cellulose pyrolysis. *Fuel*. 2001;80:1809–1817.
13. Banyasz JL, Li S, Lyons-Hart J, Shafer KH. Cellulose pyrolysis: the kinetics of hydroxyacetaldehyde evolution. *J Anal Appl Pyrolysis*. 2001;57:223–248.
14. Antal MJ, Friedman HL, Rogers FE. Kinetics of cellulose pyrolysis in nitrogen and steam. *Combust Sci Technol*. 1980;21:141–152.
15. Várhegyi G, Szabó P, Mok WSL, Antal MJ Jr. Kinetics of the thermal decomposition of cellulose in sealed vessels at elevated pressures. Effect of the presence of water on the reaction mechanism. *J Anal Appl Pyrolysis*. 1993;26:159–174.
16. Boutin O, Ferrer M, Lédé J. Radiant flash pyrolysis of cellulose—evidence for the formation of short life time intermediate liquid species. *J Anal Appl Pyrolysis*. 1998;47:13–31.
17. Lédé J, Blanchard F, Boutin O. Radiant flash pyrolysis of cellulose pellets: products and mechanisms involved in transient and steady state conditions. *Fuel*. 2002;81:1269–1279.
18. Lédé J. The cyclone: a multifunctional reactor for the fast pyrolysis of biomass. *Ind Eng Chem Res*. 2002;39:893–903.
19. Boutin O, Ferrer M, Lédé J. Flash pyrolysis of cellulose pellets submitted to a concentrated radiation: experiments and modeling. *Chem Eng Sci*. 2002;57:15–25.
20. Wooten JB, Seeman JI, Hajaligol MR. Observation and characterization of cellulose pyrolysis intermediates by C-13 CPMAS NMR. A new mechanistic model. *Energy Fuels*. 2004;18:1–15.
21. Yang H, Yan R, Chen H, Zheng C, Lee DH, Liang DT. In-depth investigation of biomass pyrolysis based on three major components: hemicellulose, *cellulose and lignin*. *Energy Fuels*. 2006;20:388–393.
22. Svenson J, Pettersson JBC. First pyrolysis of the main components of birch wood. *Combust Sci Technol*. 2004;176:977–990.
23. Gómez CJ, Manyà JJ, Velo E, Puigjanaer L. Further applications of a revisited summative model for kinetics of biomass pyrolysis. *Ind Eng Chem Res*. 2004;43:901–906.
24. Miller RS, Bellan J. A generalized biomass pyrolysis model based on superimposed cellulose, hemicellulose and lignin kinetics. *Combust Sci Technol*. 1997;126:97–137.
25. Miller RS, Bellan J. Tar yield and collection from the pyrolysis of large biomass particles. *Combust Sci Technol*. 1997;127:97–118.
26. Morf P, Hasler P, Nussbaumer T. Mechanisms and kinetics of homogeneous secondary reactions of tar from continuous pyrolysis of wood chips. *Fuel*. 2002;81:843–853.
27. Evans RJ, Milne TA. Molecular characterization of the pyrolysis of biomass. I. Fundamentals. *Energy Fuels*. 1987;1:123–137.
28. Müller-Hagedorn M, Bockhorn H, Krebs L, Müller U. A comparative kinetics study on the pyrolysis of three different wood species. *J Anal Appl Pyrolysis*. 2003;68–69:231–249.
29. Di Blasi C, Lanzetta M. Intrinsic kinetics of isothermal xylan degradation in inert atmosphere. *J Anal Appl Pyrolysis*. 1997;40–41:287–303.
30. Di Blasi C. Comparison of semi-global mechanisms for primary pyrolysis of lignocellulosic fuels. *J Anal Appl Pyrolysis*. 1998;47:43–64.
31. Manyà JJ, Velo E, Puigjanaer L. Kinetics of biomass pyrolysis: a reformulated three-parallel-reactions model. *Ind Eng Chem Res*. 2003;42:434–441.
32. Várhegyi G, Antal MJ Jr, Jakab E, Szabó P. Kinetic modeling of biomass pyrolysis. *J Anal Appl Pyrolysis*. 1997;42:73–87.
33. Kersten SRA, Wang X, Prins W, van Swaaij WPM. Biomass pyrolysis in a fluidized bed reactor. I. Literature review and model simulations. *Ind Eng Chem Res*. 2005;44:8773–8785.
34. Wang X, Kersten SRA, Prins W, van Swaaij WPM. Biomass pyrolysis in a fluidized bed reactor. II. Experimental validation of model results. *Ind Eng Chem Res*. 2005;44:8786–8795.
35. Hosoya T, Kawamoto H, Saka S. Pyrolysis behaviors of wood and its constituent polymers at gasification temperature. *J Anal Appl Pyrolysis*. 2007;78:328–336.
36. Hosoya T, Kawamoto H, Saka S. Influence of inorganic matter on wood pyrolysis at gasification temperature. *J Wood Sci*. 2007;53:351–357.
37. Hosoya T, Kawamoto H, Saka S. Cellulose-hemicellulose and cellulose-lignin interactions in wood pyrolysis at gasification temperature. *J Anal Appl Pyrolysis*. 2007;80:118–125.
38. Sagehashi M, Miyasaka N, Shishido H, Sakoda A. Superheated steam pyrolysis of biomass elemental components and Sugi (Japanese cedar) for fuels and chemicals. *Bioresour Technol*. 2006;97:1272–1283.
39. Hasegawa I, Fujisawa H, Sunagawa K, Mae K. Quantitative prediction of yield and elemental composition during pyrolysis of wood biomass. *J Jpn Inst Energy*. 2005;84:46–52 (in Japanese).
40. Schwanninger M, Rodrigues JC, Pereira H, Hinterstoisser B. Effects of short-time vibratory ball milling on the shape of FT-IR spectra of wood and cellulose. *Vib Spectrosc*. 2004;36:23–40.

Manuscript received May 19, 2008, and revision received Aug. 23, 2008.